

# Neocortical simulation for epilepsy surgery guidance: Localization and intervention

William W. Lytton, Samuel A. Neymotin, Jason C. Wester, and Diego Contreras

**Abstract** New surgical and localization techniques allow for precise and personalized evaluation and treatment of intractable epilepsies. These techniques include the use of subdural and depth electrodes for localization, and the potential use for cell-targeted stimulation using optogenetics as part of treatment. Computer modeling of seizures, also individualized to the patient, will be important in order to make full use of the potential of these new techniques. This is because epilepsy is a complex dynamical disease involving multiple scales across both time and space. These complex dynamics make prediction extremely difficult. Cause and effect are not cleanly separable, as multiple embedded causal loops allow for many scales of unintended consequence. We demonstrate here a small model of sensory neocortex which can be used to look at the effects of microablations or microstimulation. We show that ablations in this network can either prevent spread or prevent occurrence of the seizure. In this example, focal electrical stimulation was not able to terminate a seizure but selective stimulation of inhibitory cells, a future possibility through use of optogenetics, was efficacious.

---

William W. Lytton  
SUNY Downstate, Kings County Hospital, Brooklyn, NY 11203 e-mail:  
billl@neurosimsim.downstate.edu

Samuel A. Neymotin  
SUNY Downstate, Brooklyn, NY 11203 e-mail: samn@neurosimsim.downstate.edu

Jason C. Wester  
University of Pennsylvania Medical School, Philadelphia, Pennsylvania 19104 e-mail:  
jcwester@gmail.com

Diego Contreras  
University of Pennsylvania Medical School, Philadelphia, Pennsylvania 19104 e-mail:  
diegoc@mail.med.upenn.edu

## 1 Localization and microlocalization

Localization has traditionally been a particular focus of diagnosis and treatment in neurology and neurosurgery. Localization for an internist generally offers only a few choices, *e.g.*, determining whether dyspnea is pulmonary or cardiological, or more rarely due to anemia. In the clinical neurosciences, the many interactions make localization far more difficult.

With the transition from pneumoencephalography and like medieval testing methods to modern noninvasive imaging techniques, localization as a diagnostic skill began to seem a thing of the past. Nowadays, large pathological entities declare themselves onscreen in a way that was only possible postmortem in the past. However, growing information about neurotransmitters, receptors, cellular function and network connectivity now enables detailed microlocalization, based on levels of analyses, organized across the various omes.[8, 9, 10]

Given the sensitivity and centrality of the target organ, neurosurgeons have long been leaders in the development of minimally invasive surgery. However, in current epilepsy practice, neurosurgical intervention is used as a last resort, after pharmacological treatment has failed. The resulting surgeries are at that point often relatively large resections, typically a portion of one medial temporal lobe.[6, 40] Infrequent, but even more dramatic, is the use of hemispherectomy in treatment of childhood epilepsies.

On the other hand, microlocalization is used in the preparation for cortical epilepsy surgery, where subdural electrode grids are placed in order to define specific site of seizure origin.[16] In addition, personalized medicine is here available via interventions that have been customized to the individual patient's brain. The grids are used to probe the brain for "eloquent" areas, different in detail in each patient, that should be spared in order to reduce postoperative deficits.[17] Neocortical resection are then carefully targeted based on these data.

A still less invasive, albeit generally less successful, alternative has been the use of multiple subpial transections to isolate epileptogenic zones.[2, 26, 33, 39] Subpial transections are also sometimes done as an accompaniment to resection.[35] Still less invasive is the use of electrical shock as a modality of treatment. The most successful of these are remote vagal stimulation devices.[32] However, local electrical stimulation is also being tried in an attempt to prevent or abort seizures.[7, 15, 18, 29] The use of demand pacemaking and demand defibrillation in the heart provides an encouraging precedent for this approach.

Discoveries in basic science will in the future make possible a number of alternative focal interventions in addition to electrical stimulation. For example, one could imagine transient focal application of receptor blockers directly in brain tissue, use of prolonged electrical fields to inactivate an area,[31] or focal transient cooling to reduce activity in a particular brain region.[27] An additional possibility is now arising from the new field of optogenetics.[37] This technology allows certain classes of neurons to be targeted for insertion

of ion channels which can then triggered by coherent light. This then allows one to produce transient activation or inactivation of one class of cells on demand.

**Complexity in multiscale modeling:** Microlocalization of disease and personalization of treatment both require an ability to make predictions. Currently, these predictions are necessarily made using simple assumptions about cause and effect: this area is pathological; it is creating disease; we will remove it and the patient will be better. We are all aware that this approach ignores the many complex interactions in the brain. Loops within loops of interaction provide an extremely wide range of pathophysiological manifestations.

The problem is that the brain is a dynamical system.[25] Dynamics is the field that studies states that change in time. Traditionally, these states were position and velocity, and dynamics was the study of motion. In medicine, dynamics adds to studies of physical motion of body and tissue, studies of changes in concentrations (*e.g.*, drugs, ions, proteins) and counts (*e.g.*, CBC, complete blood count). In neurobiology, we add a focus on the dynamics of signaling up from the microscopic level of synapses to the level of interactions across brain areas measured by EEG (electroencephalogram) or fMRI (functional magnetic resonance imaging).

Prediction in dynamical systems is notoriously difficult.[28] In dynamical systems, A pushes on B at the same time as B pushes on A. Meanwhile, subsystems of A may be interacting with subsystems of B both directly, and via a third system C. Perhaps one of the best studied dynamical systems is the economy, whose EEGs are the stock market indices. Here we are all familiar with interventions that lead to unintended consequences through activation of a previously unrecognized causal loop deep in the system. Sometimes such a vital causal loop can be identified post-hoc; sometimes it is never discovered. Additionally, chaos theory has taught us that small causes can have large effects.[1, 4, 38] In the brain, as in the economy, computer simulations can be used to attempt detailed predictions in advance of treatment interventions.

**Dynamics occur across many levels:** The common comparison of the brain to a computer, though in many ways useful, obscures vast differences in dynamical complexity. To pick one level, synaptic dynamics are more complex than the binary dynamics of transistors. At the level of the neuron, further analog dynamics provide a rich substrate for calculation. It has been argued that the individual neuron may parallel a computer CPU in terms of processing power.[30] Remarkably, the computational capacity of the individual neuron remains unknown.

Multiple spatial scales are also available for diagnosis and therapy:

Level	Testing	Treatments
Brain	Neuropsychological	Behavioral/rehab therapies
Areas	fMRI, EEG,PET	Resections
Networks	ECoG	Focal ablations/MPT
Cells	Histological pathology	Optogenetics
Molecules	Blood and CSF levels	AEDs

The use of antiepileptic drugs (AEDs) in the post-surgical patient represents the interaction of an intervention at the pharmacological level with alterations that have been produced at the network or area levels. Multiscale interactions involve scaling across time as well as space. Brain remodeling due to development or other plasticity over years interacts with interventions that take place at a particular time. Following a resection, the rest of the brain will adapt in way that may produce the reemergence of seizures after a several year seizure-free period.[34, 41]

## 2 Simulation methods

Simulations were run using NEURON.[5, 12] The full model is available on ModelDB (<https://senselab.med.yale.edu/ModelDB>). The single neuron model is an extension of an integrate-and-fire unit simulated in an event-driven fashion with state variables calculated only at the time of input events. Added complexity provided adaptation, bursting, depolarization blockade, and voltage-sensitive NMDA conductance.[21, 22, 23, 24]

Each neuron had a membrane voltage level state variable  $V_m$  and a resting membrane potential  $V_{RMP}$ . After synaptic input events, if  $V_m$  crossed spiking threshold  $V_{TH}$ , the cell would emit an action potential and enter an absolute refractory period, lasting  $\tau_{refrac}$  ms, during which it could not fire. Following the action potential, an after-hyperpolarization voltage state variable  $V_{ahp}$  was set and then subtracted from  $V_m$ .  $V_{ahp}$  decayed exponentially with time-constant  $\tau_{ahp}$  to 0. Depolarization blockade was simulated using a  $V_{block}$  value, above which no firing was allowed. Relative-refractory period was simulated after an action potential by increasing the threshold,  $V_{TH}$ , by  $W_{RR} \cdot (V_{block} - V_{TH})$ , where  $W_{RR}$  was a unitless weight parameter.  $V_{TH}$  then decayed exponentially to its baseline value with time constant  $\tau_{RR}$ .

Each cell had a voltage state-variable associated with a synapse type,  $V_{syn}$ , one for each of excitatory AMPA, NMDA, and two inhibitory GABA<sub>A</sub>s, which simulated GABA<sub>A</sub> at soma (fast time-constant) and GABA<sub>A</sub> at dendrite (slower time-constant). Synaptic inputs were simulated by step-wise changes in  $V_{syn}$  and then added to the cell's  $V_m$  level. To allow for dependence on  $V_m$ , synaptic inputs changed  $V_{syn}$  by  $\delta V = w_{syn} \cdot (1 - \frac{V_m}{E_{syn}})$ , where  $w_{syn}$  is the synaptic weight and  $E_{syn}$  is the reversal potential, relative to  $V_{RMP}$ .  $E_{syn}$  took the following values (in mV): AMPA 65, NMDA 90, GABA<sub>A</sub> -15.  $w_{syn}$  was positive for excitatory synapses and negative for inhibitory synapses. NMDA synapses also had an additional voltage-dependent scaling factor based on physiology.[13, 14] For all synapses, after synaptic in-

put events,  $V_{syn}$  decayed exponentially towards 0 with time constant  $\tau_{syn}$  with values AMPA 20 ms, NMDA 300 ms, somatic GABA<sub>A</sub> 10 ms, dendritic GABA<sub>A</sub> 20 ms. Synaptic weights were constant between a given set of populations. Dendritic synapses (AMPA, NMDA, dendritic GABA<sub>A</sub>) utilized delays chosen from a uniform distribution ranging from 3–5 ms, while somatic synapses (somatic GABA<sub>A</sub>) had delays ranging from 1.8–2.2 ms.

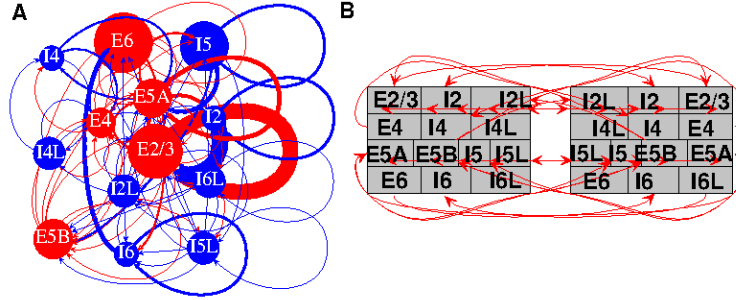


**Fig. 1** Network structure and wiring. **A.** *Intracolumnar* connections. Red are excitatory populations (circles, size represents population size) and projections (lines, width represents projection strength); blue for inhibitory. Directed wiring is red for excitatory and blue for inhibitory connections. Cell types are E (excitatory) or I (inhibitory), followed by layer number (2 represents 2/3) and an additional letter for cell subsets: L=low-threshold spiking cells; Layer 5 has two E cell subpopulations: 5a,5b. **B.** *Intercolumnar* connections. Layers are here explicitly represented as would be seen in an anatomical view.

Baseline wiring and number of cells per layer were similar to those used previously (Fig. 1).[28] 13 cell types were arranged in 4 layers: 2/3, 4, 5, and 6. Interneurons were parameterized as fast-spiking (FS) or low-threshold spiking (LTS) interneurons. FS and LTS interneurons utilized somatic and dendritic GABA<sub>A</sub> synapses, respectively. The following cell types were included: E2, I2, I2L, E4, I4, I4L, E5a, E5b, I5, I5L, E6, I6, and I6L. E (I) represent excitatory (inhibitory) cells, and the number following the cell-type represents the layer, *i.e.*, E2 represents pyramidal cells in layers 2/3. I6 represents FS interneurons in layer 6, and I6L represents LTS interneurons in layer 6. E5a and E5b are two subtypes of pyramidal neurons present in layer 5, with different connectivity patterns.[3, 11, 36] Although both wiring and component specifications remain incompletely understood, there is growing knowledge on which we base our models.

Fig. 1A gives a graph theoretic view of intracolumnar wiring, with connectivity depicted by red arrows for excitatory and blue for inhibitory connections. Intergroup connectivity density within the column is moderate (43%; 72 out of 169 possible connections for the 13 cell groups). Total E→E connections were 88%; E→I connections 25%; I→E connections 45%; I→I con-

nections 34%. All populations have self-connections (note that these are not connections from a cell to itself but from cells in a group to different cells in the same group). In this depiction, the influence of the cell populations for a single column are arrayed circumferentially according to their importance. The central position is taken by the excitatory population in L2/3. Arrayed around the center are other groups in different layers. Each layer has 2 types of inhibitory cells with slightly different dynamics. L5 also has 2 types of excitatory cells.

Fig. 1B shows the layered structure of neocortex giving *intercolumnar* group-to-group wiring between neocortical columns, an anatomical view comparable to sectioning normal to the brain surface. These intercolumnar projections tend to be confined within each layer and are strongest across L2/3 and L5. Lateral excitatory projections synapse onto both excitatory and inhibitory cells (feedforward inhibition). There are again 169 possible connections, but the connection probability is  $\sim 7.7\%$  (13/169), far lower than within column. Although all projection pathways are excitatory, most project onto inhibitory cells and thereby produce feedforward inhibition, largely laterally to the same layer across columns. An additional major lateral inhibitory projection goes from E5b $\rightarrow$ I2L. E5, the main output layer, is also the source of intercolumnar feed-forward excitatory connections, including E5b $\rightarrow$ E2 and connections from both E cell groups in layer 5. There is also relatively minor intercolumnar feed-forward excitation between E2 cells.

### 3 Simulation results

Fig. 2A shows a view looking down at a chain of paired columns. Connections between columns are to nearest neighbor with no wrap-around. This  $7 \times 2$  architecture was chosen as the minimal model that would reliably produce sequential activation with spread of seizure activity.

Baseline activity in the 7 pairs of columns is arrayed top to bottom pairwise across 250 ms of time in Fig. 2B. Only the excitatory cell groups are shown; they are color coded as indicated on the right with each symbol representing a single spike in one cell. Spikes cannot be individually seen since most are obscured by other spike in this highly compressed raster. The 7 paired columns (left to right) are represented as rows in the raster. Activity here is regular, being driven both by interconnects and by ongoing random stimulation of all cells.

This simulation was run on the edge of an epileptiform transition, where high recurrent excitation can allow random coincident activation to produce spontaneous seizures. Such a seizure is shown in Fig. 2B. Aberrant activity spread can be traced back to the time indicated by the arrow with initiation of increased activity in the third and fourth rows from top. Following initiation, there was a brief period of spread before the first population burst occurred. Thereafter, activity was tightly grouped in bursts of  $\sim 32$  ms duration separated by a comparable interval for a population spike rate near 15 Hz. Contrasting the single burst at lower right with the normal activity just

above demonstrates that a high proportion of E2/3 (black) and E5A (green) fire during an epileptic population burst. This activity shift has an analogy to a phase change, where stimulation at a single location produces a dramatic alteration in dynamics in the network as a whole.

**Blocking activation by focal ablation** In the control simulation, Fig. 3A, seizure activity occurred throughout the chain. The simulated local field potentials (LFPs) at top show high amplitude recurrent activity at each of the 14 columns in the network. Breaking the column chain by eliminating a single pair in the center necessarily prevented seizure spread across the chain. This did not however prevent a seizure from occurring spontaneously in one of the remaining sections (Fig. 3). The seizure now occurred in the top 3 pairs but could not spread to the lower 3 pairs. As a minimal intervention, this “ablation” would be more akin to a subpial transection than to a surgical resection. A larger ablation (2 adjacent pairs) entirely prevented seizure initiation (Fig. 3C). The amount of epileptogenic tissue was now reduced sufficiently that the critical mass required for seizure initiation was not now present. This suggests the possibility of using a “debulking” procedure to reduce epileptogenesis while preserving tissue.

**Blocking activation by focal stimulation** In prior simulations, we have noted that a strong single activation could stop or prevent a seizure by si-

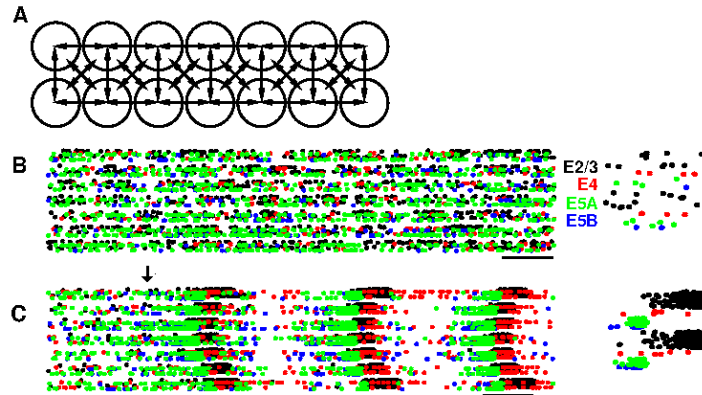


**Fig. 2** **A.** Tangential view looking down to show connectivity of columns in the  $2 \times 7$  model. **B** Raster plots of baseline activity. Each dot (color code to right) represents a single spike from an excitatory cell. Scale bar 25 ms is time of detail at right, taken from lowest trace. Note that each  $y$  location is a different cell. **C** Transition to epileptic activity.

multaneously activating all cells and causing them to become simultaneously refractory.[19, 20] This situation is comparable to the spontaneous occurrence of an interictal spike and supports the hypothesis that such spikes, pathognomonic for seizure disorders, might be protective. We therefore looked at the efficacy of focal stimulation as a method for preventing seizure spread using a  $2 \times 2$  column model (Fig. 4). The control simulation produced population burst activity at about 12 Hz (Fig. 4A).

We were not able to produce either stimulation seizure stoppage or stimulation seizure prevention in the present simulation after trying various phases and strengths of stimulation. Instead, stimulation either had no effect or increased the rate of seizure activity. In Fig. 4B, stimulation immediately after the first cycle (arrow) increased the frequency of the seizure to 16 Hz. The reasons for this failure of seizure abortion by stimulation in the present simulation had to do with the strength of recurrent NMDA activation, with activity carried across at a subthreshold level through continuing NMDA ac-

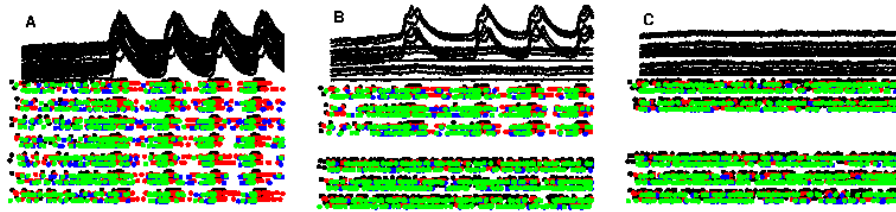


**Fig. 3** Reduce spread or eliminate seizure in  $2 \times 7$  model. Each trace is 500 ms in duration. LFPs at top, shown in order of the rasters at bottom, start slightly after the rasters due to an edge effect.

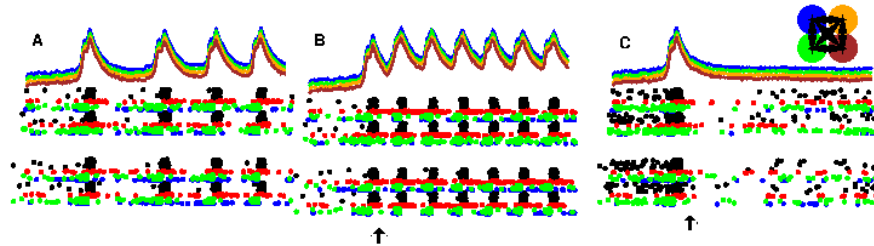


**Fig. 4** Stimulation to stop seizure. Each trace 500 ms. LFP color code at upper right, (unrelated to color coding of cell types in rasters)

tivation. Note that the difference between different types of simulations in this respect is not surprising and might be expected to correspond to differences among different seizure generation in different brain areas and by different underlying pathologies in different patients. Hence we would predict that some patients will have seizures with vulnerability to stimulations which would not be effective in others. We further predict that patients who are resistant to this form of seizure stoppage would also show fewer interictal spikes.

We next tried directed stimulation of inhibitory cells alone (Fig. 4C). In a patient, such selective activation would have to be performed using optogenetics, a process that allows selected cell groups to be activated via laser light through use of light-sensitive ion channels that are introduced only into cells that have been targeted previously for insertion of channelrhodopsin. In the present simulation, this procedure was able to prevent seizure continuation, resulting in normal activity patterns following a brief period of inactivity. The active repolarization associated with activation of inhibitory inputs into the cells allowed them to reinstate the magnesium blockade of NMDA receptors and prevented the activity carry-over observed in (Fig. 4B).

**Modeling as a predictor for surgery:** In this paper we have demonstrated how microsurgical procedures could be simulated using a relatively simple multiscale network model. Although the modeling shown here is primarily at the network level, it is built atop models of neuronal electrophysiology which are in turn based on models of synapses and ion channels. Therefore, we could add pharmacology to these models by, for example, reducing the propensity for cell bursting as a consequence of treatment with phenytoin. Eventually, we would want to assess the interactions of surgical therapy, pharmacotherapy and brain plasticity.

With future advances in neuroimaging as well as electrode recording, specific models would be developed for the individual patient in order to optimize treatment strategy. Far more complex models will be needed to provide a personalized approach to the individual patient's brain dynamics, brain wiring and brain pathology.

**Acknowledgements** Research supported by NIH R01MH086638 and DARPA N66001-10-C-2008.

## References

1. Babloyantz, A., Destexhe, A.: Low-dimensional chaos in an instance of epilepsy. *Proc Nat Acad Sci* **83**, 3513–3517 (1986)
2. Benifla, M., Otsubo, H., Ochi, A., Snead, O., Rutka, J.: Multiple subpial transections in pediatric epilepsy: indications and outcomes. *Childs Nerv Syst* **22**, 992–998 (2006)
3. Brown, S., Hestrin, S.: Intracortical circuits of pyramidal neurons reflect their long-range axonal targets. *Nature* **457**(7233), 1133–1136 (2009)
4. Buonomano, D.: Harnessing chaos in recurrent neural networks. *Neuron* **63**, 423–425 (2009)

5. Carnevale, N., Hines, M.: *The NEURON Book*. Cambridge University Press, New York (2006)
6. Clusmann, H., Kral, T., Gleissner, U., Sassen, R., Urbach, H., Blmcke, I., Bogucki, J., Schramm, J.: Analysis of different types of resection for pediatric patients with temporal lobe epilepsy. *Neurosurgery* **54**, 847–859 (2004)
7. Cohen-Gadol, A., Stoffman, M., Spencer, D.: Emerging surgical and radiotherapeutic techniques for treating epilepsy. *Curr Opin Neurol* **16**, 213–219 (2003)
8. Crampin, E., Halstead, M., Hunter, P., Nielsen, P., Noble, D., Smith, N., Tawhai, M.: Computational physiology and the physiome project. *Exp Physiol* **89**, 1–26 (2004)
9. Duarte, N., Becker, S., Jamshidi, N., Thiele, I., Mo, M., Vo, T., Srivas, R., Pals-son, B.: Global reconstruction of the human metabolic network based on genomic and bibliomic data. *Proc Nat Acad Sci* **104**, 1777–1782 (2007)
10. Dubitzky, W.: Understanding the computational methodologies of systems biology. *Brief Bioinform* **7**, 315–317 (2006)
11. Groh, A., Meyer, H., Schmidt, E., Heintz, N., Sakmann, B., Krieger, P.: Cell-type specific properties of pyramidal neurons in neocortex underlying a layout that is modifiable depending on the cortical area. *Cereb Cortex* **20**(4), 826–836 (2010)
12. Hines, M., Carnevale, N.: NEURON: a tool for neuroscientists. *The Neuroscientist* **7**, 123–135 (2001)
13. Jahr, C., Stevens, C.: Voltage dependence of NMDA-activated macroscopic conductances predicted by single-channel kinetics. *J Neurosci* **10**(9), 3178–3182 (1990)
14. Jahr, C., Stevens, C.: A quantitative description of NMDA receptor-channel kinetic behavior. *J Neurosci* **10**(6), 1830 (1990a)
15. Kossoff, E., Ritzl, E., Politsky, J., Murro, A., Smith, J., Duckrow, R., Spencer, D., Bergey, G.: Effect of an external responsive neurostimulator on seizures and electrographic discharges during subdural electrode monitoring. *Epilepsia* **45**, 1560–1567 (2004)
16. Lesser, R., Crone, N., Webber, W.: Subdural electrodes. *Clin Neurophysiol* **121**, 1376–1392 (2010)
17. Lesser, R., Crone, N., Webber, W.: Using subdural electrodes to assess the safety of resections. *Epilepsy Behav* **20**, 223–229 (2011)
18. Lesser, R., Kim, S., Beyderman, L., Miglioretti, D., Webber, W., Bare, M., Cysyk, B., Krauss, G., Gordon, B.: Brief bursts of pulse stimulation terminate afterdischarges caused by cortical stimulation. *Neurology* **53**, 2073–2081 (1999)
19. Lytton, W., Hellman, K., Sutula, T.: Computer network model of mossy fiber sprouting in dentate gyrus. *Epilepsia – AES Proceedings* **37 S. 5**, 117 (1996)
20. Lytton, W., Hellman, K., Sutula, T.: Computer models of hippocampal circuit changes of the kindling model of epilepsy. *Artificial Intelligence in Medicine* **13**, 81–98 (1998)
21. Lytton, W., Neymotin, S., Hines, M.: The virtual slice setup. *J Neurosci Methods* **171**, 309–315 (2008b)
22. Lytton, W., Omurtag, A.: Tonic-clonic transitions in computer simulation. *J Clin Neurophysiol* **24**, 175–181 (2007)
23. Lytton, W., Stewart, M.: A rule-based firing model for neural networks. *Int J Bioelectromagnetism* **7**, 47–50 (2005)
24. Lytton, W., Stewart, M.: Rule-based firing for network simulations. *Neurocomputing* **69**(10-12), 1160–1164 (2006)
25. Milton, J.: Epilepsy as a dynamic disease: a tutorial of the past with an eye to the future. *Epilepsy Behav* **18**, 33–44 (2010)
26. Morrell, F., Whisler, W., Bleck, T.: Multiple subpial transection: a new approach to the surgical treatment of focal epilepsy. *J Neurosurg* **70**, 231–239 (1989)

27. Motamedi, G., Salazar, P., Smith, E., Lesser, R., Webber, W., Ortinski, P., Vicini, S., Rogawski, M.: Elimination of epileptiform activity by cooling in rat hippocampal slice epilepsy models. *Epilepsy Res* **70**, 200–210 (2006)
28. Neymotin, S., Lee, H., Park, E., Fenton, A., Lytton, W.: Emergence of physiological oscillation frequencies in a computer model of neocortex. *Frontiers Comput Neurosci* **5** (2011)
29. Osorio, I., Frei, M., Manly, B., Sunderam, S., Bhavaraju, N., Wilkinson, S.: An introduction to contingent (closed-loop) brain electrical stimulation for seizure blockage, to ultra-short-term clinical trials, and to multidimensional statistical analysis of therapeutic efficacy. *J Clin Neurophysiol* **18**, 533–544 (2001)
30. Polsky, A., Mel, B., Schiller, J.: Computational subunits in thin dendrites of pyramidal cells. *Nat Neurosci* **7**, 621–627 (2004)
31. Richardson, K., Schiff, S., Gluckman, B.: Control of traveling waves in the mammalian cortex. *Phys Rev Lett* **94**, 028,103 (2005)
32. Rutecki, P.: Anatomical, physiological, and theoretical basis for the antiepileptic effect of vagus nerve stimulation. *Epilepsia* **31S2**, S1–S6 (1990)
33. Schramm, J., Aliashkevich, A., Grunwald, T.: Multiple subpial transections: outcome and complications in 20 patients who did not undergo resection. *J Neurosurg* **97**, 39–47 (2002)
34. Schulz, R., Hoppe, M., Boesebeck, F., Gyimesi, C., Pannek, H., Woermann, F., May, T., Ebner, A.: Analysis of reoperation in mesial temporal lobe epilepsy with hippocampal sclerosis. *Neurosurgery* **68**, 89–97 (2011)
35. Spencer, S., Schramm, J., Wyler, A., Connor, M., Orbach, D., Krauss, G.: Multiple subpial transection for intractable partial epilepsy: an international meta-analysis. *Epilepsia* **43**, 141–145 (2002)
36. Steriade, M.: Neocortical cell classes are flexible entities. *Nat Rev Neurosci* **5**(2), 121–134 (2004)
37. Tonnesen, J., Sorensen, A., Deisseroth, K., Lundberg, C., Kokaia, M.: Optogenetic control of epileptiform activity. *Proc Nat Acad Sci* **106**, 12,162–12,167 (2009)
38. TY, L., Yorke, J.: Period three implies chaos. *Amer. Math. Monthly* **82**, 985–992 (1975)
39. Wyler, A.: Recent advances in epilepsy surgery: temporal lobectomy and multiple subpial transections. *Neurosurgery* **41**, 1294–1301 (1997)
40. Wyler, A., Hermann, B., Somes, G.: Extent of medial temporal resection on outcome from anterior temporal lobectomy: a randomized prospective study. *Neurosurgery* **37**, 982–990 (1995)
41. Yogarajah, M., Focke, N., Bonelli, S., Thompson, P., Vollmar, C., McEvoy, A., Alexander, D., Symms, M., Koepp, M., Duncan, J.: The structural plasticity of white matter networks following anterior temporal lobe resection. *Brain* **133**, 2348–2364 (2010)